technical transactions

No. 2025/026

mechanics

Paradigm

High-symmetry-point dispersion sensitivity analysis of quasi-Rayleigh waves in periodic half-spaces

Łukasz Doliński

lukasz.dolinski@pg.edu.pl | https://orcid.org/0000-0002-9814-4269

Department of Manufacturing Systems, Faculty of Mechanical Engineering and Robotics, AGH University of Krakow; Department of Biomechatronics, Faculty of Electrical and Control Engineering, Gdańsk University of Technology

Bartłomiej Piwowarczyk

bartlomiej.piwowarczyk@agh.edu.pl | https://orcid.org/0009-0005-8432-2852

Paweł Paćko

pawel.packo@agh.edu.pl | https://orcid.org/0000-0002-8962-9969

Department of Manufacturing Systems, Faculty of Mechanical Engineering and Robotics, AGH University of Krakow

Daniel Torrent

dtorrent@uji.es | https://orcid.org/0000-0001-7092-7360

Institut de Noves Tecnologies de la Imatge, Universitat Jaume I

Scientific Editor: Grzegorz Filo, Cracow University of Technology
Technical Editor: Aleksandra Urzędowska, Cracow University of Technology Press
Typesetting: Małgorzata Murat-Drożyńska, Cracow University of Technology Press

Received: November 4, 2025
Accepted: December 4, 2025

Data Availability Statement: All relevant data are within the paper and its Supporting Information files.

Competing interests: The authors have declared that no competing interests exist.

Funding: This research was supported by the DYNAMO project (101046489), funded by the European Union.

Citation: Doliński, Ł., Piwowarczyk, B., Paćko, P., Torrent, D. (2025). High-symmetry-point dispersion sensitivity analysis of quasi-Rayleigh waves in periodic half-spaces. Technical Transactions, e2025026. https://doi.org/10.37705/TechTrans/e2025026

Abstract

This work investigates the sensitivity of surface-wave dispersion characteristics in periodic phononic structures with two types of scatterers: cylindrical pillars and finite-depth circular holes. We develop high-fidelity finite element models of square unit cells with Bloch boundary conditions and analyse the effect of geometric parameters (diameter and height/depth) on eigenfrequencies at a Brillouin zone high-symmetry point. A global sensitivity analysis based on the one-factor-at-a-time method is performed to quantify parameter influence and non-linear interactions. The results show that, for pillar-type structures, the pillar height dominates the dynamic response, while for hole-type structures both diameter and depth have comparable effects. Large geometric variations lead to mode reordering and narrow frequency separations, which is critical for bandgap-oriented optimisation. The approach outlines a route towards tunable phononic platforms for wave-based imaging applications.

Keywords: periodic structures, sensitivity analysis, Rayleigh waves, dispersion

1. Introduction

Metamaterials are mechanical structures with a characteristic periodic pattern that exhibit unusual dynamic behaviours not observed in nature (Hussein et al., 2014). By adjusting the geometric parameters of the structure, metamaterials can be designed to demonstrate negative Poisson's ratio, adjustable stiffness, high damping capacity, or customised wave propagation characteristics. These unique properties, particularly the existence of frequency bandgaps, have led to increased interest in periodic structures in recent years, making them the subject of intensive research. They are of great interest in various fields of science and industry, including materials science and mechanical engineering (Sun and Zhou, 2025; Guenneau et al., 2007). The basis of every metamaterial is its unit cell – a structural element repeated periodically in space – which determines the overall mechanical response of the structure. The topology, geometry, and material distribution in this unit cell determine its dynamic properties, including its frequency characteristics (Capolino, 2009; Engheta and Ziolkowski, 2006). The design of metamaterials can be viewed through the selection of geometric and material properties of the unit cell, e.g. via multi-criteria optimisation strategies (Yu et al. 2018 ; Behrou et al., 2020). However, optimising the shape of a structure, especially in terms of its dynamic characteristics, is challenging in many respects. First, the relationship between the parameters of the elementary cell and the dynamic responses is often highly nonlinear and multidimensional (Capolino, 2009; Krushynska et al., 2023). Furthermore, the structural analysis of a three-dimensional elasticity problem is computationally intensive. Implementing a direct optimisation approach, especially for a case of a large number of design parameters, may be time-consuming in terms of computation or insufficient in terms of the expected accuracy of the results, e.g. convergence problems may arise due to the presence of local minima or parameter interactions. Another issue that needs to be addressed in the context of the problem of defining the objective function and possible problems that may occur at the stage of optimisation calculations is that, in the case of large changes in the decision variables, a situation may occur in which neighbouring vibration modes swap. This is particularly significant in an area where several modes have almost the same frequencies. It is therefore crucial to examine and understand the relationship between the geometry of the samples and their dynamic properties. The solution is to perform a sensitivity analysis that will provide information on which parameters have the strongest influence on the response, thus guiding model simplification/surrogate modelling and optimisation. It is critical to note that the relationship between the geometrical features of the structure and its spectral response is nontrivial and nonlinear.

Sensitivity analysis is a fundamental tool in engineering, allowing the determination of how variations in system parameters affect the response of interest (Saltelli et al., 2008). In mechanical systems, such analyses help to identify dominant parameters, reduce model complexity, and guide optimisation or uncertainty quantification. As a consequence, the key design parameters can be selected and their influence on the response can be evaluated. In general, the analysis can be performed once a model of the system is available, regardless of its type. The process of building a numerical model can be complex, especially when the relationships between inputs and outputs are uncertain and/or random. Sources of uncertainty can include both insufficient knowledge of the system and measurement errors, but also the influence of random phenomena. In such cases, the model can be treated as a *black box*, in which the exact relationships between the inputs and outputs of the system are unknown. The process of sensitivity analysis is a study that identifies how the changes in the model results can be attributed to different parameters in the input data. It involves exploring a multidimensional space of input variables by cyclically solving a model for alternative initial parameters and determining sensitivity measures based on

https://doi.org/10.37705/TechTrans/e2025026

statistical quantities, thus determining which set of inputs has a dominant effect on the given outputs (Campolongo et al., 2007). Sensitivity analysis enables the identification and better understanding of the relationships between input and output variables in the model without the need to examine all possible solution cases. This makes it possible not only to look for errors in the model but also to identify parameters that have a negligible impact on the system. By identifying redundant parts of the model structure, it is possible to simplify the model, which translates directly into reduced design costs. Sensitivity analysis is also often an integral part of the optimisation process, in particular for the selection of the relevant optimisation parameters (Castillo et al., 2008; Allaire et al., 2004).

Sensitivity analysis methods can be divided into local and global approaches (Saltelli et al., 2019). Local methods (gradient-based) may not account for nonlinear interactions between parameters. Global methods (e.g., the Sobol indices or the Morris method) provide a more comprehensive picture of the relationships between the studied parameters, but they require additional computational effort. One of the simplest and most common sensitivity analysis approaches is the one-factor-at-a-time method. It involves solving the model for one changing input variable while keeping the remaining parameters at their base values. After completing the assumed number of cycles, the tested variable is restored to the base value and the procedure is repeated in the same way for the next parameter. The advantage of this approach is that any change observed in the model output will result from a change in a specific input variable. The sensitivity of the model to changes in the input parameter can be determined using statistical measures. Depending on the number and variability range of the inputs, the parameter space can contain a large number of points to be investigated. To avoid the necessity of checking all possible combinations of the inputs, a number of statistically driven samples (trajectories) are selected and evaluated to compute the sensitivity measures (Campolongo et al., 2011). The key element of the current work is to investigate and understand relations between the geometrical and material features of the samples and their dynamic properties, and to select those parameters that are of particular importance to the design. Consequently, the main goal of this study is to investigate and understand the relationships between the geometric features and dynamic properties of the unit cell of a phononic structure, in an assumed pillar or hole configuration. We investigated the proposed structures with the aim of identifying a model suitable for practical imaging applications. In particular, our long-term objective is to develop a phononic platform that enables the excitation of arbitrarily shaped displacement patterns at the surface of the structure, which could serve as a basis for future wave-based imaging devices. Two factors are crucial in this context: the group velocity and the density of modes. By selecting a wavenumber at the boundary of the Brillouin zone, we potentially obtain both zero group velocity and a high density of modes, which can be tailored through the parameters identified in the sensitivity analysis.

The aim of this work is therefore to: (i) develop a numerical model of a periodic structure; (ii) perform global sensitivity analyses to identify the dominant design parameters; and (iii) discuss physical implications and provide guidelines for parametric optimisation.

2. Methodology

2.1. Model definition

In this work, we consider square unit cells (in the $x - y$ plane) of a half-space (i.e. semi-infinite in the z direction), with one of two scatterers: (a) a pillar with a circular cross-section, and (b) a circular hole of finite depth (Liu et al., 2000). The geometry of both samples are shown in Fig. 1(a). The same model can be used where positive height renders a pillar and negative height results in a hole.

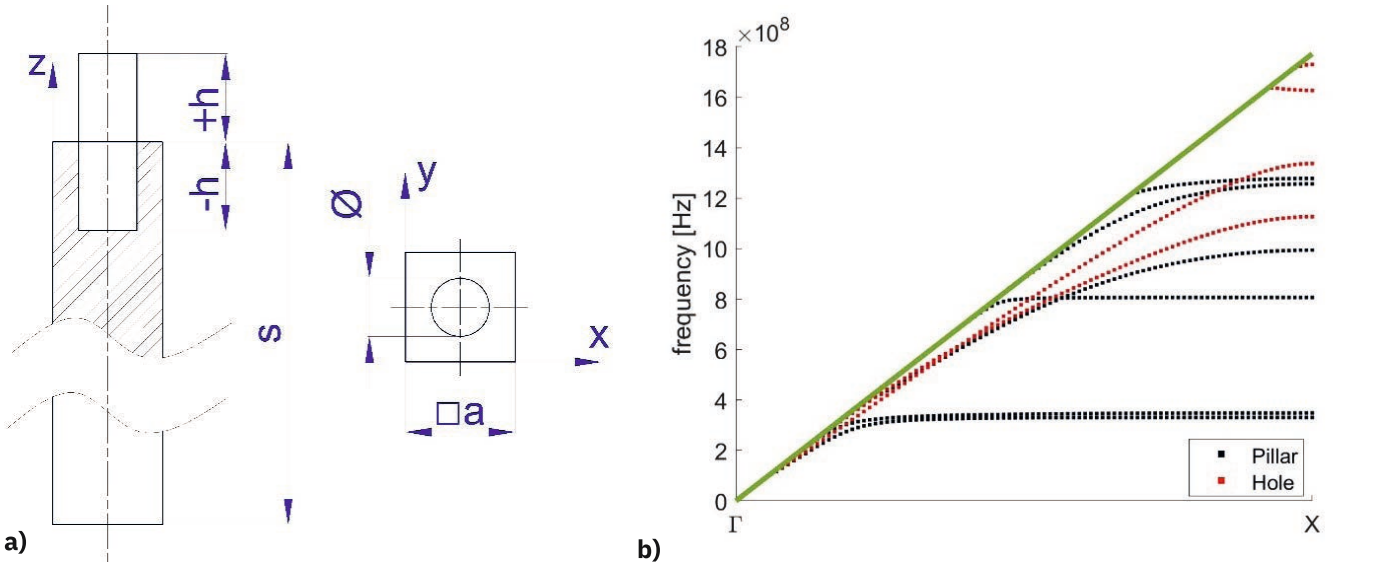

Fig. 1. a) Side view of a single unit cell along with the top view and the assumed coordinate system. The scatterer, i.e. pillar or hole, can be geometrically parametrized by a positive or negative value of height (+/-h), respectively. b) An example of the dispersion diagram for a unit cell with a pillar (black markers) and a hole (red markers) for the Γ - X path in the Brilluoiun zone. The green line denotes the sound cone (own elaboration)

We treat pillars and holes separately during the modelling process as the height values close to zero result in weak scattering properties of pillars and holes.

For a numerical model of the half-space, the thickness is finite and has to be sufficiently large compared to the unit cell side length to avoid coupling of surface waves to the lower surface. After conducting a series of tests, we assumed that a thickness 20 times greater than the unit cell edge length is sufficient to study surface waves at the selected high-symmetry point. The actual thickness that was used in experiments is much larger, to eliminate recording of the waves that are reflected from the bottom surface. We rejected the typical choice of non-reflecting boundary conditions to avoid complex natural frequencies. For the chosen thickness we used fixed boundary conditions and performed some additional actions, to ensure we analyze only surface modes. First, for a given Bloch wavenumber, we computed the limiting frequencies, below which the downward-propagating wavevector component is imaginary, so this component is evanesecent. In addition, we introduced modes matching algorithm to detect only waves of interest. The remaining dimensions are also defined relative to the unit cell edge length. The exact values of geometric parameters for both cases are presented in Tab. 1, along with the ranges of parameters subject to modification during the sensitivity analysis process.

The Bloch periodic boundary conditions were applied to the vertical faces of the model (i.e. assuming periodicity in the $x - y$ plane). The bottom surface of the substrate was fixed. Initially, an alternative approach with a Perfectly Matched Layer (PML) below the homogeneous substrate layer was implemented and tested. It was found, however, that this choice resulted in a number of numerical

Table 1. Geometric properties of the unit cell: * in the x–y plane; ** in the z-axis dimension; *** in the x–y plane with the coordinate system centred at (0,0) of the component (i.e. the bottom left corner, see Fig. 1). (own elaboration)

quantity	symbol	base value [μm]	tested range [μm]
edge length *	a	1.5	const.
substrate depth **	s	20a = 30	const.
pillar diameter *	ϕ	0.7a = 1.05	0.525:1.47
pillar height*	h	0.7a = 1.05	0.525:2.6
hole diameter *	ϕ	0.7a = 1.05	0.105:1.365
hole depth*	h	0.7a = 1.05	0.105:4.2
pillar/hole centre position ***	x_p, y_p	0.5a = 0.75	const.

https://doi.org/10.37705/TechTrans/e2025026

issues, e.g. complex eigenvalues and multiple artificial modes (including multiple modes localised close to the PML layer). With the assumed substrate layer depth, the selection of the fixed boundary condition allows one to find the wave modes of interest — modes with the most energy localised at the surface — and compare them more easily.

The Bloch boundary condition of the for

$$u(\boldsymbol{x},\boldsymbol{k}) = e^{i\boldsymbol{k}\boldsymbol{x}}\tilde{u}(\boldsymbol{x},\boldsymbol{k}) \tag{1}$$

was applied to the vertical faces of the unit cell, where $u(\boldsymbol{x},\boldsymbol{k})$ is the displacement field, $\tilde{u}(\boldsymbol{x},\boldsymbol{k})$ is the periodic part of the displacement field, $e^{i\boldsymbol{k}\boldsymbol{x}}$ is the phase factor, and $\boldsymbol{k} = (k_x, k_y)$ is the wavevector in the x–y plane (Khelif and Adibi, 2015). Please note that in the sensitivity analysis we study only the case of $\boldsymbol{k} = (k_x, 0)$ at the X point, i.e. $k_x = \pi/a$, where a is the unit cell size. Moreover, modes at the Brillouin zone boundaries may display intriguing properties, e.g. localisation or zero group velocity. Our assumptions result in the following relation when comparing Bloch waves of adjacent unit cells:

$$u(x+a, y, k_x) = e^{ik_x a}u(x, y, k_x), \tag{2}$$

which for $k_x = \pi/a$ gives

$$u(x+a, y, k_x) = -u(x, y, k_x), \tag{3}$$

and

$$u(x+2a, y, k_x) = u(x, y, k_x) \tag{4}$$

so the Bloch function has a period of two unit cells in the x direction.

A common characteristic that is related to periodic media is dispersion relation of the frequency and Bloch wavenumber. Fig. 1b) shows dispersion relations for a unit cell with a pillar and a hole. The horizontal axis shows the dimensionless wavenumber $q = \frac{ka}{\pi}$ and the vertical axis shows frequency in Hz. The fixed diameter $\phi = 1$ μm and height (depth) $h = 1.5$ μm for the pillar (hole) were chosen for the plots. The dashed line present at both plots denotes the limiting frequency for the surface modes. Comparing curves in Fig. 1b) it can be seen that more surface modes are present for the unit cell with the pillar. In addition, no complete bandgap is observed for the frequency range presented.

2.2. Sensitivity measures

For the presented studies, we consider the one-factor-at-a-time method. In this approach, we attempt to evaluate the sensitivities of the output parameters to the inputs by screening the parameter space in a statistical sense. The method proposed in 1991 by Morris is particularly well suited for models with a large number of uncertain factors and/or when the model calculations are expensive. Sensitivity analysis is performed for a given number j of model input variables, examining their effects and interactions on the output parameters. Each variable can take values in the assumed (predefined) range. Thus, the set of model input parameters under study forms a multidimensional space, including all possible combinations of available values for the parameters. By moving by a fixed jump value sequentially through all coordinates in the j-dimensional space, a single trajectory is created, which is a set of model inputs based on which the model outputs are determined. Thanks to this information, it is possible to track changes in the output parameters of the model with a specific change in a given input variable. It involves calculating, for each input signal, a series of incremental coefficients, called elementary effects (EE), as

$$EE_i = \frac{f(x_1,\ldots,x_i+\Delta,\ldots,x_j)-f(x)}{\Delta}, \Delta = \frac{1}{p-1} \tag{5}$$

where $f(x)$ is the model response for successive steps of the single trajectory, j is the number of input variables, Δ is the fixed (normalised) discretisation step of the sensitivity grid, and p is the number of levels for each variable in the j-dimensional space.

The number of evaluated elementary effects (number of trajectories) should be large enough to cover the j-dimensional space of input variables within the assumed ranges of variability. In order to assess the overall significance of individual model parameters, two sensitivity indices are calculated based on elementary effects. The first parameter is the mean μ or modified mean μ^*, given by Eq. (6), which estimates the overall effect of the factor on the outcome. The second sensitivity measure is the standard deviation σ, given by Eq. (7), which estimates the ensemble of higher-order effects of the factor, i.e. non-linear and/or due to interactions with other factors.

$$\mu_j^* = \frac{1}{N}\sum_{i=1}^{N}|EE_i|, \Delta = \frac{1}{p-1} \tag{6}$$

$$\sigma_j = \sqrt{\frac{1}{N-1}\sum_{i=1}^{N}\left(EE_i-\mu_j^*\right)^2}, \Delta = \frac{1}{p-1} \tag{7}$$

where N is the number of trajectories.

A large mean indicates a large factor effect. A large σ indicates that the effect depends strongly on the values of other factors, suggesting their non-linear interaction. Fig. 2 shows a diagram of the interpretation of sensitivity measures for the results of sensitivity analysis as the coefficient of variation σ/μ^* (Morris, 1991; Saltelli, et al. 2008; Campolongo et al., 2007).

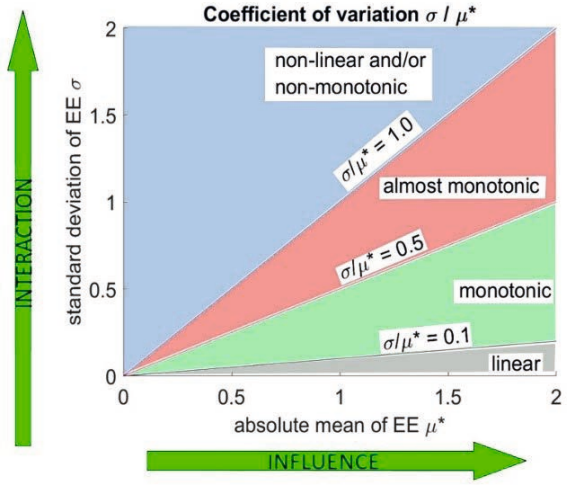

Fig. 2. Graphical illustration of the sensitivity measures space μ^* and σ (own elaboration)

2.3. Numerical procedure

The model and analysis procedure outlined in earlier sections were implemented using a combined framework of finite element software and Matlab. Detailed geometric features of the models are presented in Sec. 2.1. The material used for all the calculations is polycrystalline silicon. We assumed linear and isotropic mechanical properties in the numerical model. This choice can be justified by taking an assumption of very small, nanometer-sized, and randomly oriented grains. The exact values we used are: Young's modulus E = 160 GPa, Poisson's

https://doi.org/10.37705/TechTrans/e2025026

ratio $\nu = 0.22$, and density $\rho = 2320\ \mathrm{kg/m^3}$. Second-order tetrahedral serendipity elements were selected for discretisation to reduce the effects of excessive stiffening. Before selecting specific mesh properties (minimum and maximum element sizes and mesh rates), a convergence analysis was performed (Sigmund and Jensen 2003). The analysis consisted of solving the eigenvalue problem for the lowest 50 eigenvalues for multiple models. The mesh parameters investigated were (1) the minimum and (2) maximum element size, (3) maximum element growth rate, (4) the curvature coefficient, and (5) mesh refinement around small structural features. The models considered have simple geometry, which allowed us to significantly improve the accuracy of the results by adjusting the element size. The last three parameters were used for adjustments.

The convergence analysis was conducted in two stages. First, the maximum and minimum element sizes were modified, with the last three parameters (coefficients (3–5)) remaining constant (1.25, 0.5 and 0.6, respectively). We compared models in pairs where a model with the finer mesh had two times smaller minimum and maximum element sizes. The relative error of natural frequencies was then calculated. The results of the finer model were taken as a reference. The relative error was calculated as:

$$e_n = \frac{\left| f_{nc} - f_{nf} \right|}{f_{nf}} \tag{8}$$

where e_n is the relative error of the n^{th} mode, and f_{nc} and f_{nf} are the n^{th} natural frequencies of the coarser and finer model, respectively. The aim was to find a pair of models that results in a maximum relative error below 1%. The finer model was then taken as a reference model for the next step. In the next step, we selected models with the mesh coarser than the mesh of the reference model. The aim was to find a rough approximation of the model parameters that results in natural frequencies with an error not exceeding 3% when compared to the reference model. The parameters found by employing the above-mentioned procedure (presented in Tab. 2) were used in the sensitivity analysis.

Table 2. Mesh parameters for models used in the convergence analysis (own elaboration)

Model	Max. element size [μm]	Min. element size [μm]	Max. element growth rate	Number of elements
Reference	0.20	0.02	1.25	139458
Final	0.80	0.08	1.50	2056

With the convergence analysis finished, the sensitivity analysis followed. It was performed using a set of developed Matlab functions that allow for the generation, modification, simulation, and post-processing of the results. The results are determined for a high-symmetry X point of the spectral properties and for a limited number of eigenvalues (up to 50). We found that within this range, we could find a set of eigenvalues with the desired properties, i.e. multiple surface-localised modes in the selected frequency range.

3. Results

As discussed, the sensitivity study was conducted for unit cells of two types, i.e. with pillars or holes, with the goal of examining the impact of changes in selected geometric parameters on the dispersion characteristics at the high-symmetry X point. For pillars, the impact of changes in the diameter and the height h of the pillar was examined, while for holes, changes in the diameter and the depth h of the round hole were analysed. Due to the low geometrical complexity of the numerical model and, consequently, the low computational cost, the study

used an exhaustive search method, which consisted of determining the output parameters for all possible combinations of input variables from the assumed variability ranges of the investigated parameters. For this purpose, in both cases, the two-dimensional space of variables and h was divided into 25 intervals in each direction. This resulted in 26 constant values of the diameter and 26 corresponding constant height or depth values from the specified range, which gave 676 pairs of values forming the basis of the input parameters of the numerical model. The ranges of changes in geometric parameters are presented in Tab. 1. The change in frequency (for a fixed $k_x = \pi/a$) and the frequency separation of adjacent vibration modes within the selected frequency range were taken as the output variables.

3.1. Wave propagation in a pillar-structured half-space

Fig. 3a) presents a summary of numerical calculations performed for an elementary cell with a pillar. Each surface represents the frequency distribution for a given mode across the full range of input variables analysed, for $\boldsymbol{k} = (\pi/a, 0)$. The parameters marked as $\Delta\phi$ and Δh denote incremental values resulting from the division of the respective parameter ranges into $p = 26$ equal levels in accordance with the assumptions of the Morris screening method. As can be seen, the effect of changing the and h parameters on the frequency is not identical for all modes, which causes mode planes to interpenetrate and change their positions in the spectrum. To better illustrate this phenomenon, Fig. 3b) shows the contours of the planes belonging to specific modes, after their identification. Generally, it can be stated that the parameter h has the greatest influence on the change in frequency. Intuitively, the greatest decrease in frequency occurred for the largest values of pillar height and the base diameter value. This effect is a direct consequence of multiple modes of different types, i.e. longitudinal and bending, for long beam-like structures.

This observation is consistent with the variation coefficient calculations shown in Fig. 4(a), where each marker represents the variation coefficient for one mode, taking into account the sensitivity to changes in diameter (black markers) and height (red markers), respectively.

Analysis of the results presented in Fig. 4 allows the following conclusions:

- all variation coefficients are close to or above the line $\sigma/\mu^* = 1$, which, according to Fig. 2, indicates a non-linear and/or non-monotonic dependence of the natural frequency value on the variables,
- a change in the height of the pillar has a much greater impact and interaction on the result of the calculated model than a change in the diameter,

Fig. 3. Frequency distribution for an elementary cell with a pillar in the full space of input variables for the first six modes, $\Delta\phi$ and Δh denote incremental values resulting from the division of the respective parameter ranges into $p = 26$ equal levels (own elaboration)

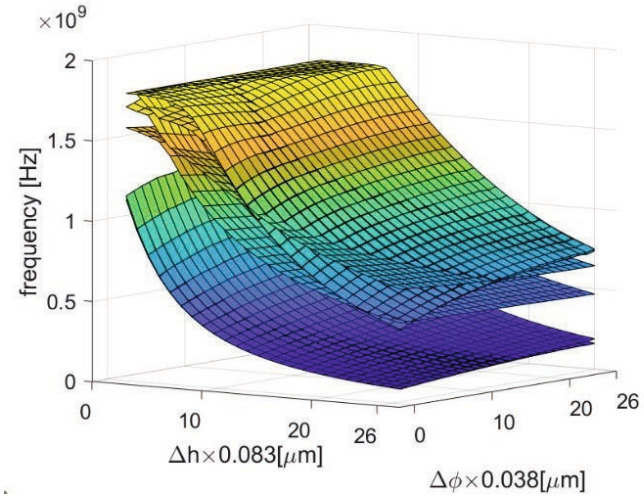

a) Frequency distribution (mode identification required)

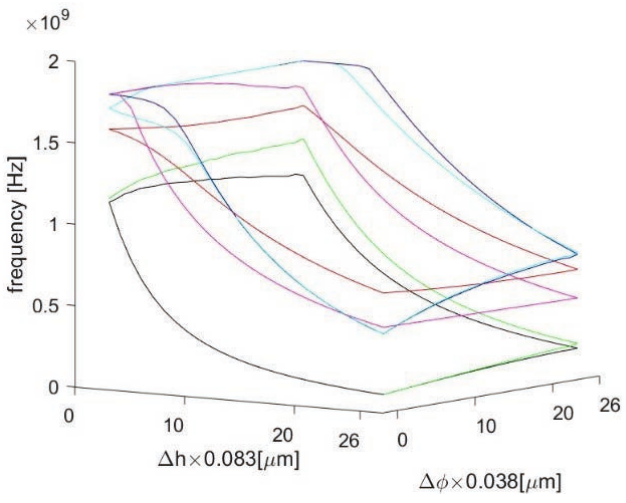

b) Interpenetration of planes of individual vibration modes

https://doi.org/10.37705/TechTrans/e2025026

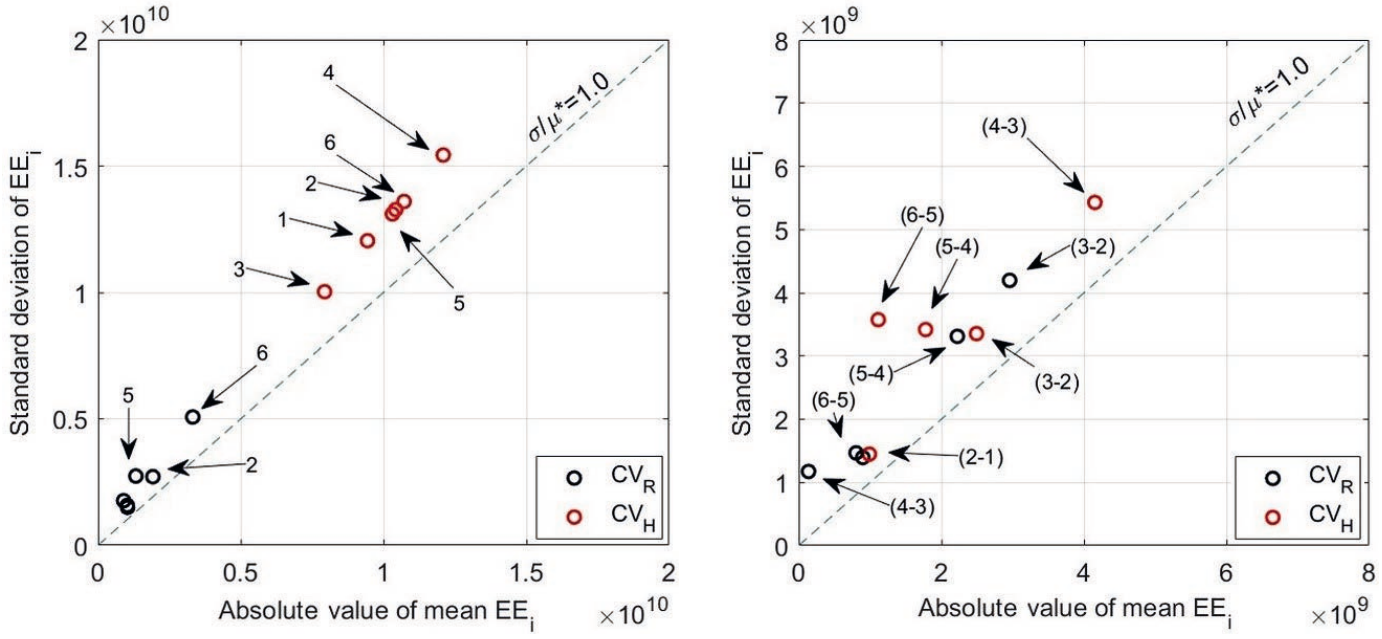

a) CV for eigenfrequencies

b) CV for eigenfrequency differences

Fig. 4. Results of elementary effect calculations using the Morris method for a unit cell with a pillar for the first six modes. CV_R is the variation coefficient associated with the diameter change, while CV_H is the variation coefficient associated with the height change (own elaboration)

- there is a noticeably different sensitivity of individual modes to changes in the geometric parameters of the pillar. Modes 1, 3, and 4 are practically insensitive to changes in the pillar diameter, and respond mainly to changes in its height. Meanwhile, modes five and six are clearly sensitive to variations in both geometric parameters. The difference in the sensitivity of individual modes can also be seen in Fig. 3, where for the fifth and sixth modes we observe a shift of the frequency surface below the surfaces of the third and fourth modes.

These conclusions are further strengthened by analysing the variation coefficients determined for frequency differences (adjacent modes), presented in Fig. 4(b). Analysis of this parameter can be useful in the context of optimisation for uniform mode distribution in the frequency spectrum or maximising bandgap widths within a specific frequency range. As can be seen, the frequency differences between individual mode pairs (1–2 and 5–6) are minor, and the effect of changes in geometry (especially diameter) on frequency changes is comparable. This results in minimal possibilities for modifying the frequency difference between these modes. This fact is worth considering when defining the optimisation objective function.

3.2. Wave propagation in a hole-structured half-space

Subsequently, analogous calculations were performed for a unit cell with a circular hole. Fig. 5 presents a summary of the results. Each surface represents the frequency distribution for a given mode across the full range of input variables analysed. In this case, all modes examined are sensitive to changes in the parameters and h, with both parameters having an approximately equal effect on the frequency of a given mode.

Fig. 6a) and 6b) show the frequency variation coefficients and frequency differences calculated for the model with a blind hole, respectively. Each marker represents the variation coefficient for a single mode, taking into account sensitivity to changes in input parameters (ϕ – black markers, h – red markers).

The analysis of the distribution of variation coefficients for all inputs leads to the following conclusions:

- as in the case of a pillar, all variation coefficients are close to or above the line $\sigma/\mu^* = 1$ (nonlinear and/or non-monotonic relationship between natural frequency values and variables),
- a change in the diameter of the hole has a greater impact and interaction on the result of the calculated model than a change in depth for a specific mode,
- natural frequencies with higher values are less sensitive to changes in input variables.

Fig. 5. Frequency distribution for an elementary cell with a hole in the full space of input variables for the first six modes, $\Delta\phi$ and Δh denote incremental values resulting from the division of the respective parameter ranges into $p = 26$ equal levels (own elaboration)

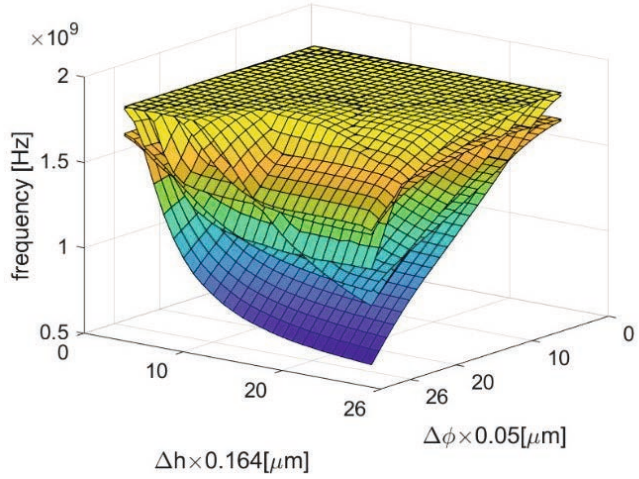

a) Frequency distribution (mode identification required)

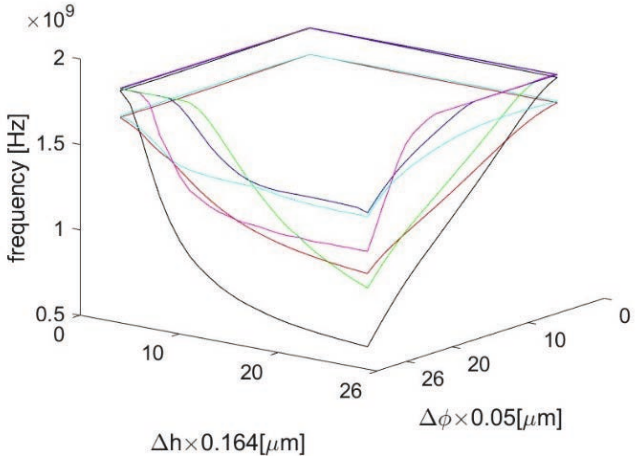

b) Interpenetration of planes of individual vibration modes

Fig. 6. Results of elementary effect calculations using the Morris method for a unit cell with a hole for the first six modes. CV_R is the variation coefficient associated with the diameter change, while CV_H is the variation coefficient associated with the depth change (own elaboration)

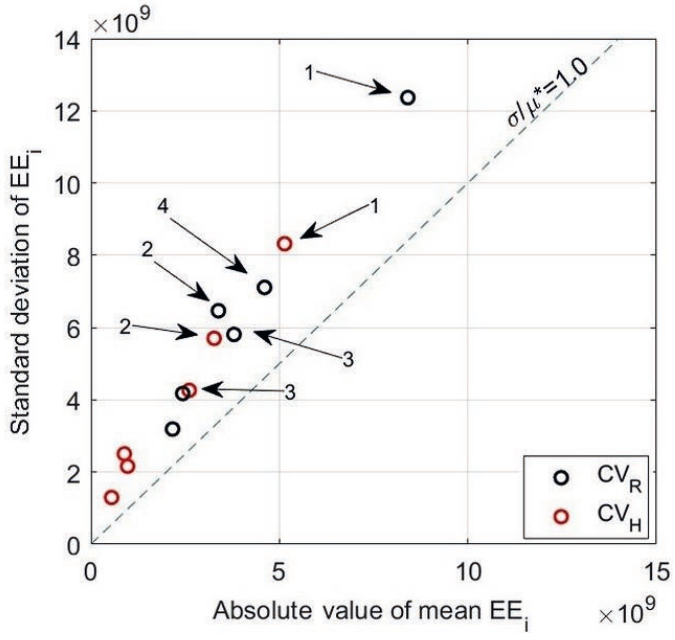

a) CV for eigenfrequencies

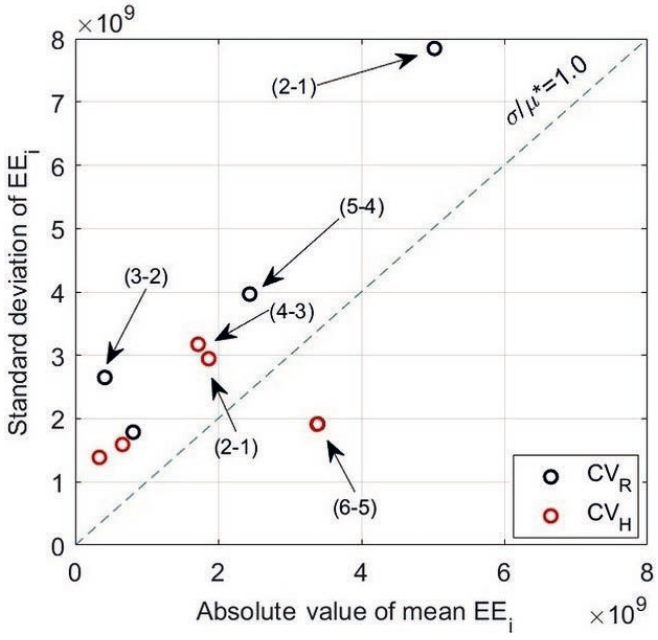

b) CV for eigenfrequency differences

https://doi.org/10.37705/TechTrans/e2025026

4. Conclusions

The work presented here focuses on the sensitivity analysis of two phononic structures: one with a cylindrical pillar and one with a circular hole of finite depth. The diameter and height/depth were selected as the parameters subject to change. Due to the limited number of unit cell geometry parameters examined, it was decided to search the entire assumed variable space. The analysis of the results obtained was carried out using elementary effect calculations with the Morris method (onefactor-at-a-time). The sensitivity analysis was performed based on changes in natural frequencies within a defined frequency range and changes in frequency differences for adjacent modes, for a fixed wavevector corresponding to a high-symmetry point in the dispersion space. The analyses were carried out using the finite element method and Matlab, and employed libraries that allow their coupling. This approach was selected to allow automatic model generation, performing simulations, and post-processing of the results. This combination of software tools allows for automatic analysis of hundreds of models required for the sensitivity analysis. The key observations and conclusions are:

- the change in the pillar height has the greatest impact on the observed frequency parameters,
- the effect of changing the pillar geometry is visible primarily at higher frequencies,
- for the hole-type scatterer, both geometric parameters affect the observed frequency characteristics; however, for a given mode, variations in the hole diameter have a noticeably stronger influence than variations in its depth,
- higher natural frequencies are less sensitive to changes in input parameters for structures with the hole,
- for both types of scatterers (pillar and hole), the interaction of geometric parameters is strongly non-linear and/or heterogeneous,
- the analysis of the frequency graph of the studied structure (Figs. 3 and 5) shows that significant changes in the values of decision variables cause the planes of individual vibration modes to cross over for both pillar and hole structures. For specific optimisation purposes, it is therefore necessary to identify the modes and take this information into account in the optimisation process. Relying only on the frequency values carries the risk that the optimisation process will not achieve the intended goal.
- the manufacturing of real samples is always subject to uncertainty regarding the final dimensions, both due to manufacturing tolerances and the occurrence of potential unintentional manufacturing errors. Conducting a sensitivity analysis allowed us to observe the impact of these factors on the observed dynamic parameters. The obtained results suggest that, within a small range of variations, the impact of unintentional geometric for both types of scatterers will have a negligible effect on the structure's properties

References

Allaire, G., Jouve, F., and Toader, A.-M. (2004). Structural optimization using sensitivity analysis and a level-set method. *Journal of Computational Physics 194*(1):363–393.

Behrou, R., Abi Ghanem, M., Macnider, B.C., Verma, V., Alvey, R., Hong, J., Emery, A.F., Kim, H.A., Boechler, N. (2021). Topology optimization of nonlinear periodically microstructured materials for tailored homogenized constitutive properties, *Composite Structures 266*: 113729. https://doi.org/10.1016/j.compstruct.2021.113729

Campolongo, F., Cariboni, J., and Saltelli, A. (2007). An effective screening design for sensitivity analysis of large models. *Environmental Modelling and Software 22*(10): 1509 – 1518.

Campolongo, F., Saltelli, A., and Cariboni, J. (2011). From screening to quantitative sensitivity analysis. a unified approach. *Computer Physics Communications 182*(4): 978–988.

Capolino, F. (2009). *Theory and Phenomena of Metamaterials*. Boca Raton, FL: CRC Press.

Castillo, E., M´ınguez, R., and Castillo, C. (2008). Sensitivity analysis in optimization and reliability problems. *Reliability Engineering and System Safety 93*(12): 1788–1800.

Engheta, N. and Ziolkowski, R. W. (2006). *Metamaterials: Physics and Engineering Explorations*. New York: John Wiley & Sons, Hoboken.

Guenneau, S., Movchan, A., P´etursson, G., and Anantha Ramakrishna, S. (2007). Acoustic metamaterials for sound focusing and confinement. *New Journal of Physics 9*(11): 399.

Hussein, M. I., Leamy, M. J., and Ruzzene, M. (2014). Dynamics of phononic materials and structures: Historical origins, recent progress, and future outlook. *Applied Mechanics Reviews 66*(4): 040802.

Khelif, A. and Adibi, A.U. (2015). Phononic crystals: Fundamentals and applications.

Krushynska, A.O., Torrent, D., Arag´on, A.M., Ardito, R., Bilal, O.R., Bonello, B., Bosia, F., Chen, Y., Christensen, J., Colombi, A., Cummer, S. A., Djafari-Rouhani, B., Fraternali, F., Galich, P. I., Garcia, P. D., Groby, J.-P., Guenneau, S., Haberman, M. R., Hussein, M. I., Janbaz, S., Jim´enez, N., Khelif, A., Laude, V., Mirzaali, M.J., Packo, P., Palermo, A., Pennec, Y., Pic´o, R., L´opez, M. R., Rudykh, S., Serra-Garcia, M., Torres, C.M. S., Starkey, T.A., Tournat, V., and Wright, O.B. (2023). Emerging topics in nanophononics and elastic, acoustic, and mechanical metamaterials: an overview. *Nanophotonics 12*(4): 659–686.

Liu, Z., Zhang, X., Mao, Y., Zhu, Y.Y., Yang, Z., Chan, C.T., and Sheng, P. (2000). Locally resonant sonic materials. *Science 289*(5485): 1734–1736.

Morris, M.D. (1991). Factorial sampling plans for preliminary computational experiments. *Technometrics 33*(2): 161–174.

Saltelli, A., Aleksankina, K., Becker, W., Fennell, P., Ferretti, F., Holst, N., Li, S., and Wu, Q. (2019). Why so many published sensitivity analyses are false: A systematic review of sensitivity analysis practices. *Environmental Modelling and Software 114*: 29 – 39.

Saltelli, A., Ratto, M., Andres, T., Campolongo, F., Cariboni, J., Gatelli, D., Saisana, M., and Tarantola, S. (2008). *Global Sensitivity Analysis: The Primer*. John Wiley Sons, Chichester.

Sigmund, O. and Jensen, J. S. (2003). Systematic design of phononic band-gap materials and structures by topology optimization. *Philosophical transactions. Series A, Mathematical, physical, and engineering sciences 361*(1806): 1001 – 1019.

Sun, J. and Zhou, J. (2025). Metamaterials: The art in materials science. *Engineering 44*: 145–161.

Yu, X., Zhou, J., Liang, H., Jiang, Z., and Wu, L. (2018). Mechanical metamaterials associated with stiffness, rigidity and compressibility: A brief review. *Progress in Materials Science 94*: 114–173.

https://doi.org/10.37705/TechTrans/e2025026